Switchable helical holographic structures

Suraj P. Gorkhali
Gregory P. Crawford
Maryna Yemtsova
Theo Rasing

Abstract — A 3-D array of helical structures fabricated using holographic polymer-dispersed liquid crystals (H-PDLC) is presented. Multiple coherent beams are interfered to create a constructive helical pattern which is permanently captured using the standard H-PDLC method. Films with such array of helical structures have both diffractive and circular polarization sensitive reflective properties. Iso-intensity patterns, design parameters, fabrication process, optical/electro-optical performance of these periodic helical structures are discussed along with their potential application for advanced electro-optical devices.

Keywords — *Holographic polymer-dispersed liquid crystal (PDLC), helical structure, chiral, spiral.*

1 Introduction

Circularly polarized light propagating parallel to the helical axis of an optical material results in reflection at a specific wavelength corresponding to the pitch length of the helix. The helical twist can be right or left handed. A film with a sufficient number of such helical twists formed with materials of adequate dielectric contrast completely reflects normally incident circularly polarized light. The reflected light has the same rotation direction as the helical twist while transmits the circularly polarized light with a rotation in the opposite direction. Researchers have shown that periodic helical structures in the optimized tetragonal square form have large and complete photonic bandgaps.[1,2] These helical structures have been widely investigated for color filters,[3] reflectors,[4] and circular polarizers.[5] There are plenty of examples in nature that have helical or twisted structures on the nanometer scale. Twisted-layered structures of the collagen fibers in bone,[6] spontaneously formation of a cholesteric phase in DNA,[7] a cholesteric liquid-crystalline phase in natural silk spinning processes[8] and more have been shown to exist.

One method to generate such twisted structure is by adding a chiral dopant to a nematic liquid crystal to form a cholesteric liquid-crystal (CLC) phase. The chiral molecules are not identical to their mirror image and have handedness to it. The director of the nematic phase spontaneously adopts a helical arrangement with the chiral dopant constituents in which the director **n** rotates continuously along one direction. The pitch of the helix in this case is determined by the properties and concentration of the chiral dopant. The wavelength of the reflected light by a cholesteric liquid-crystal film is between $\lambda_1 = pn_o$ and $l_2 = pn_e$, where p is the pitch of the helix and n_o and n_e are the ordinary and extraordinary refactive indices of the liquid crystal. Helical structures on the order of the wavelength of light formed by CLC and cholesteric polymers have been widely investigated for a number of applications such as low-power displays,[9] 3-D displays,[10] temperature sensors,[11] lasers,[12] and color-filter arrays.[13]

Glancing angle deposition (GLAD) is another method of creating such helical structures with a much larger dielectric contrast.[15,16] Discrete helical posts are formed by oblique-angle physical vapor deposition where the substrate tilt angle is changed continuously during vapor flux deposition. The chiral microstructure is formed as a result of shadowing effect from the rotating preformed structure. The pitch of the helix is determined by the speed of rotation. Other structures such as chevrons, helices, and zig–zag structures on a nanometer scale have been fabricated using this method.[16]

Direct laser writing (DLW) has been used to fabricate the helical photonic crystal structure.[17–20] A pulsed laser with the single-photon energy lower than the polymerization threshold of the photoresist is sharply focused on the sample to create a multiphoton point. The photoresist sample is then precisely maneuvered with a computer-controlled 3-D piezoelectric transducer stage to capture the designed structure. Using the DLW technique, Seet *et al.* demonstrated spiral structures of various parameters with photonic band gaps in the infrared region and Maxwell's lattice scaling behavior.[19]

It is possible to fabricate such helical structures in the order of the wavelength of light using a holographic method. Pang and co-workers have shown a chiral microstructure in photoresist using a holographic method.[21] The same concept can be extended to fabricate helical structures to a holographic polymer-dispersed liquid crystal (H-PDLC) to make an actively switchable helical structure. The fabrication method and electro-optical properties of microstructures using holographic methods in polymer-dispersed liquid crystals (PDLCs) are well understood.[22,23] The holographically created spiral structures have similar properties and interactions with light as the other helical structures discussed above. The morphology, optical properties,

Revised extended version of a paper presented at the 26th International Display Research Conference held September 18–22, 2006 at Kent State University, Kent, OH, U.S.A.

S. P. Gorkhali and G. P. Crawford are with Brown University, Division of Engineering, 182 Hope St., Providence, RI 02912; telephone 401/863-3049, fax -9120, e-mail: suraj_gorkhali@brown.edu.

M. Yemtsova and T. Rasing, Radboud University Nijmegen, Institute for Molecules and Materials, 6525 ED Nijmegen, The Netherlands.

and the electro-optical performance of these fabricated samples were investigated.

2 Experimental

2.1 Beam vectors

The irradiance profile generated from the interference of multiple coherent beams in a linear, isotropic medium can be generalized as the vector sum of electric fields[18]

$$\mathbf{I}(\mathbf{r}) \propto \mathbf{R}\left(\sum_{l=1}^{N}\sum_{m=1}^{N}\mathbf{E}_l\mathbf{E}_m e^{i(\mathbf{K}_l-\mathbf{K}_m)\cdot\mathbf{r}}\right) = \mathbf{R}\left(\sum_{l=1}^{N}\sum_{m=1}^{N}\mathbf{E}_l\mathbf{E}_m e^{i(\mathbf{G}_{lm})\cdot\mathbf{r}}\right), \quad (1)$$

where $\mathbf{I}$ is the resulting intensity, $\mathbf{r}$ is the spatial position vector, N is the number of coherent beams or fold symmetry, and the $\mathbf{K}$ are the wavevectors. The constructive interference point lies at the location where it satisfies the Bragg's diffraction condition $\mathbf{G}_{lm} \cdot \mathbf{r} = 2n\pi$. Six coherent, monochromatic, linearly polarized beams with the same polar angle were symmetrically distributed along the azimuthal plane creating an interference pattern consisting of high-intensity regions forming hexagonal pattern posts [Fig. 1(a)]. The lattice parameter or the separation distance between the posts can be calculated using Bragg's law:

$$d = \frac{\lambda}{\sin(\pi/3)\sin(\phi)}, \quad (2)$$

where d is the separation between the posts, λ is the wavelength of the constructive laser beams, and ϕ is the polar angle of the beams. Superposition of one additional circularly polarized beam with wave vector $\mathbf{K}_0 = k(0,0,1)$ to this configuration of six beams transforms the interference pattern of the posts to a helical spring-like structure. The helical twist in the irridance pattern results from the circularly polarized central beam and the twist depends on the handedness of the beam used. Figure 1 shows the resulting irradiance pattern from six symmetric beams compared to the helical pattern resulting from an additional central beam. The blue parts represent the high-intensity regions, while the void spaces represent low-intensity regions of the irradiance pattern. The pitch length of the discrete helical posts is determined by both the beam angle and the wavelength of the laser[21] and is given by

$$l = \frac{\lambda}{1-\cos(\phi)}, \quad (3)$$

where l is the pitch length of the helical structure. Wave vectors $\mathbf{K}_n$ and polarization vector $\mathbf{E}_n$ for all seven beams used are summarized in Table 1.

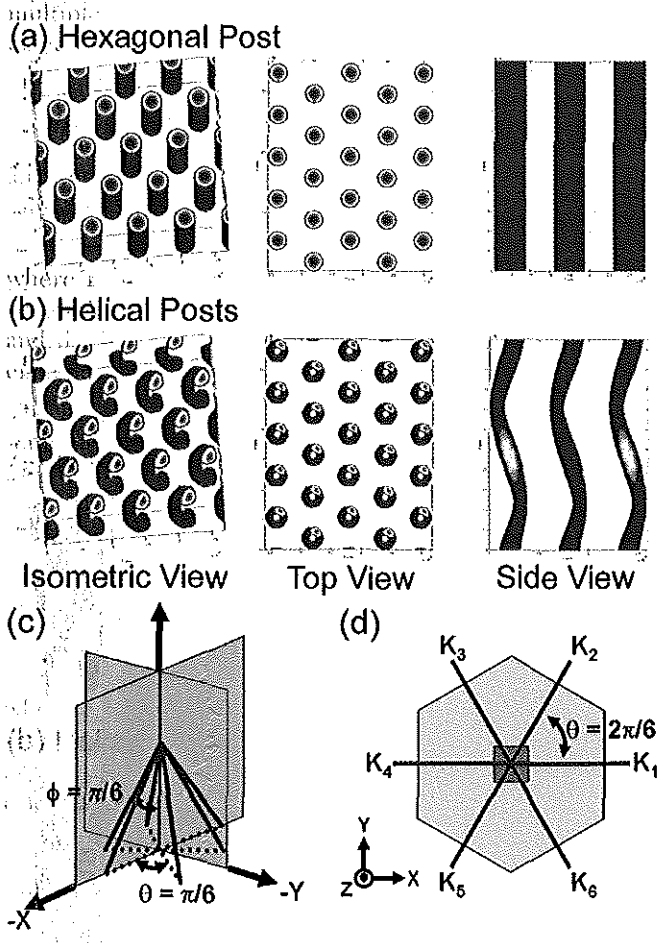

FIGURE 1 — Isometric, top, and side view of the hexagonal post irradiance pattern formed by six symmetrical beams compared to the helical post pattern formed by one addition circularly polarized beam. Beam vector arrangement of six linearly polarized beams and one circularly polarized beam used to form the patterns.

TABLE 1 — Beam vectors and polarization direction in polar and Cartesian coordinate systems.

n	(θ, ϕ)	$\mathbf{K}_n$ (K_x, K_y, K_z)	$\mathbf{E}_n$ (E_x, E_y, E_z)
1	(0°, 45°)	(.71, 0, .71)	(–.71, .00, .71)
2	(60°, 45°)	(.35, .61, .71)	(–.35, –.61, .71)
3	(120°, 45°)	(–.35, .61, .71)	(.35, –.61, .71)
4	(180°, 45°)	(–.71, 0, .71)	(.71, .00, .71)
5	(240°, 45°)	(–.35, –.61, .71)	(.35, .61, .71)
6	(300°, 45°)	(.35, –.61, .71)	(–.35, .61, .71)
7	(0°,0°)	(0, 0, 1)	(0.71, 0.71i, 0)

2.2 Irradiance pattern

A single beam from a Coherent Verdi laser operating at λ = 532 nm is split into seven beams of equal intensity (50 mW each) using a series of beam splitters. The central beam is

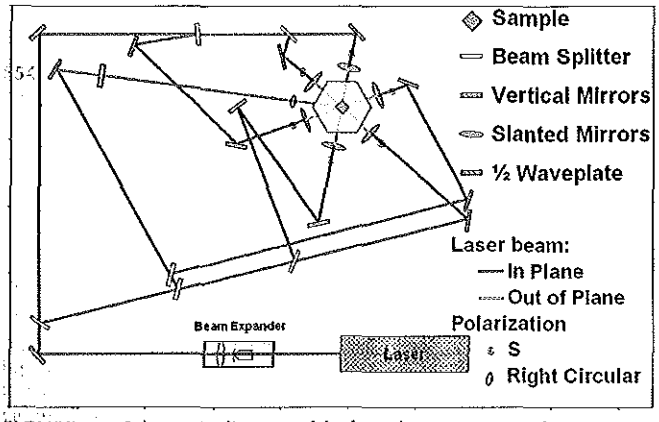

FIGURE 2 — Schematic diagram of the laser-beam setup used to generate helical interference pattern.

circularly polarized by passing it through a $\lambda/4$ waveplate and is directed towards the sample vertically. The remaining six beams were symmetrically directed to the sample at a polar angle $\phi = \pi/4$ with respect to the central beam. The wave-vector direction at which the beams are directed to the center of the sample is shown in Fig. 1(c). The schematic configuration and the picture of the optical table setup are shown in Fig. 2. The beams are arranged to minimize the path differences between any two beams.

This beam configuration results in helical pitch of 3.2 μm and a separation of 0.9 μm. The pitch of the helix decreases with increasing polar angle. It is possible to achieve wide-angle exposure for smaller pitch length by using a specially designed top-cut hexagonal prism with index-matching fluid. The circularly polarized central beam passes straight through the top cut surface and remaining six beams gets diffracted by the sidewalls of the prism to expose the holographic sample at the base of the prism. The top cut prism has been successfully used to fabricate a 3-D crystal structure[24] and an eight-fold quasi-crystal[25] using a single beam.

2.3 H-PDLC mixture

The standard H-PDLC mixture consisting of 40-wt.% nematic LC BL038, 10-wt.% surfactant, and 50-wt.% monomer mixture, and a photo-initiator was used to fabricate 20-μm-thick cells. The samples were exposed for 1 minute to the helical irradiance pattern described above. Photo-polymerization occurs at the high-intensity regions forming helical polymer posts resulting in the photo diffusion of LC to the low-intensity regions.

3 Results

3.1 Scanning electron microscopy

Morphologies of the resulting H-PDLC samples were examined with a scanning electron microscope (SEM). The samples were freeze fractured and the LC was washed to expose

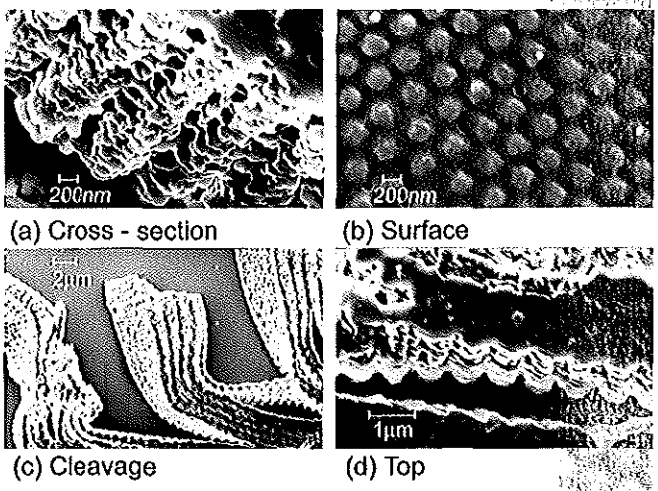

FIGURE 3 — SEM image of the (a) holographically fabricated helical posts, (b) surface morphology of the film underneath the substrate, (c) cleavage along the hexagonal boundary line forming layers of helical posts, and (d) the top view.

cross sections consisting of polymer helical posts. The SEM image in Fig. 3(a) shows an array of spiral-like microstructures. The top surface of the H-PDLC film directly beneath the glass substrate is exposed by the pealing process. The hexagonal array of helices is clearly apparent in the SEM image in Fig. 3(b). The specimen exhibits smooth cleavage planes along the layer boundaries in Fig. 3(c) exhibiting layers of separate polymer helices. The resulting morphology and the thickness of the polymer helices can be controlled by the exposure time, the LC to monomer concentration, monomer functionality, and the laser power, which in turn determines the optical and electro-optical characteristics.[26]

3.2 Diffraction pattern

The regular arrangement of helical posts in a hexagonal pattern results in a two-dimensional diffraction grating, thus a fraction of the transmitted light is diffracted. The diffraction pattern produced by a normally incident argon-ion laser (351 nm) is shown in Fig. 4(a). There are six first-order diffraction spots at a cone angle of 25° when probed with a 633-nm laser which is in agreement with the arrangement and separation of the helical posts separation mentioned above. Broadband focused white light is also diffracted and dispersed into six bright spectra shown in Fig. 4(b). The 2-D Fourier transform of the hexagonally patterned helical structure shows six discrete sharp peaks matching the diffraction pattern [Fig. 4 (inset)].

The fabricated helical pitch is of the order of 3.2 μm and corresponds to a wavelength in the infrared region. To reflect the circularly polarized light in the visible wavelength range the helical pitch length must be in the order of visible wavelengths. The period and pitch of the fabricated helical structure can be determined in many different ways. The external polar angle ϕ used for this set of experiments is $\pi/4$ which corresponds to 0.47 radian inside the sample

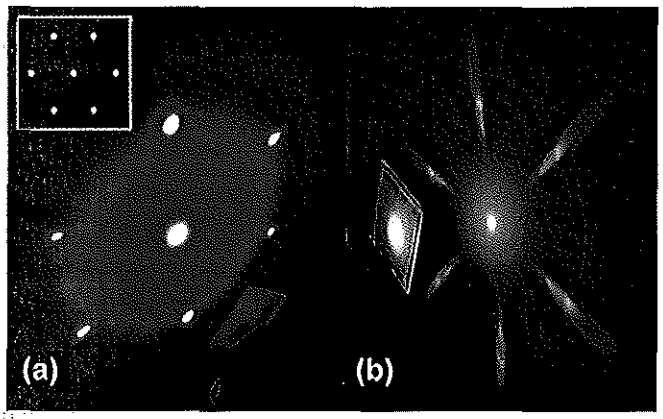

FIGURE 4 — (a) Diffraction pattern from argon-ion laser at 351 nm, and (b) from broadband focused white light. 2-D Fourier transforms along the XY plane illustrating the expected diffraction pattern (inset).

and the construction beam wavelength λ is 532 nm. Using the derived expression for period l and pitch d, the calculated period and pitch was 0.87 and 3.11 μm, respectively. The period and pitch dimensions were similar in the irradiance pattern model using vector sum of all the beams. The period can also be calculated from the diffraction-cone angle. The measured cone angle using a 633-nm He–Ne laser was 48° and the period calculated from this angle is 0.78 μm. It is also possible to optically determine the pitch of the helical structure by measuring the wavelength at which circular polarized light is reflected back. In this particular experiment, the reflection is in the IR region. Fourier transform infrared (FTIR) spectroscopy measurements in transmission and reflection mode were carried out in the range from 1000 to 5000 cm^{-1} showing a peak at 3200 cm^{-1}, but this wavenumber also corresponds to the C–H alkanes bonds common in the acrylate monomers used. The measured period and pitch from the SEM were 0.60 and 2.3 μm, respectively. The difference in the values measured in the SEM image is attributed to shrinkage and distortion during sample preparation. The optical polarization microscope images also showed hexagonal spots but the measured lattice period was twice the expected length and the intensity of the points observed varied periodically. The result strongly suggests different polarization and phase retardation across the sample and also has a repeating hexagonal pattern to it.

3.3 Electro-optical properties

When an electric field is applied across the sample, the LC molecules are aligned parallel to the applied field and the sample becomes transparent due to matched optical indices between the LC and the polymer. Both optical properties due to helical structure and hexagonal periodicity can be simultaneously varied by applying a voltage across the sample. Figure 5(a) shows that the zero-order transmission increases and the first-order diffraction intensity decreases with increasing applied voltage. The measured switching

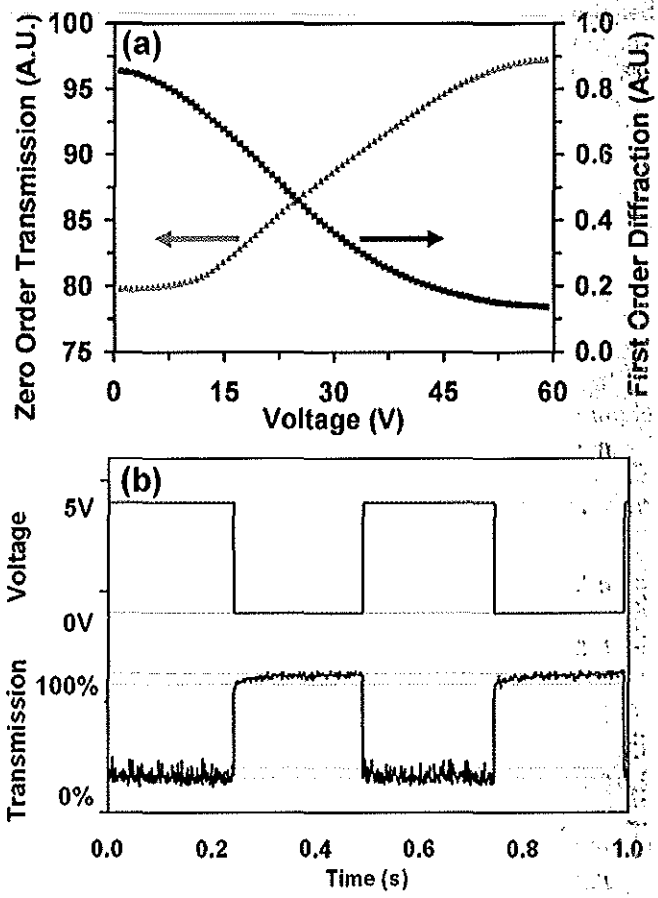

FIGURE 5 — (a) Zero-order transmission and first-order diffraction as a function of applied voltage. (b) Rise and fall time during switching, the dotted lines represent 0%, 10%, 90%, and 100% transmission.

voltage, rise time, and fall time were similar to regular H-PDLCs [Fig. 5(b)].

3.4 Decreasing pitch length

The helical pitch length decreases with increasing polar angle of the six symmetric side beams (Fig. 6). The results are plotted for the 532- and 351-nm wavelength lasers available in our lab. The helical structures investigated above were fabricated with a 532-nm green laser and the resulting pitch length was 3.21 μm. The structure had no reflective interaction with visible circularly polarized light as the pitch length was incomparable to the wavelength of visible light. The calculation shows that the pitch is within the visible range only if the angle is above 80° with a 532-nm laser. It is not possible to direct p polarized beams into the glass substrate at such wide angles due to reflection and this might require a specially designed top-cut hexagonal prism. The graph can be lowered into the visible region by using a shorter-wavelength (351 nm) laser. A UV laser with polar angle beyond 55° creates a pitch length within the visible wavelength range. The gray line at 70° in the graph shows the maximum acceptable external angle for p-polarized light

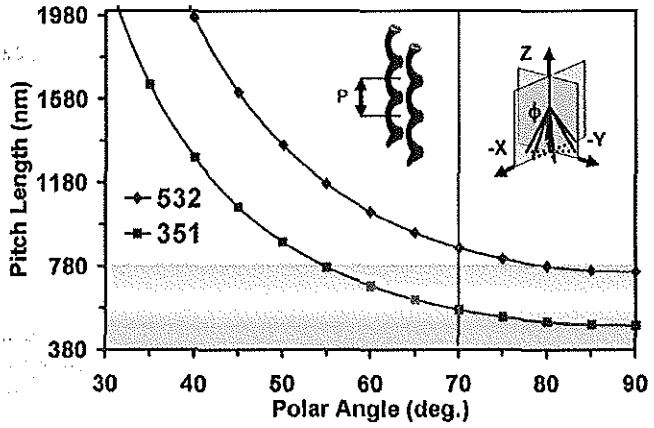

FIGURE 6 — The helical pitch length as a function of polar angle for the 351- and 532-nm system. Visible wavelength range 380–780 nm is highlighted.

(derived from Brewster's angle) to go through the glass substrate to create satisfactory H-PDLC structures. The design is still limited to pitch lengths longer than 580 nm. The helical pitch and the polar angle relationship can be reversed by directing the circularly polarized beam from the opposite direction of the sample with respect to the six other beams. When reversed, the helical pitch length decreases with decreasing polar angle, and the angle of incidence is not limited by total reflection at low angles. Using these design helical structures with much smaller pitch lengths can be fabricated as the limiting constraint is the size of the optical components.

3.5 Shrinkage

The aspect ratio (pitch:period) of the helical coils is ~4:1. At this aspect ratio, the coil looks more like a straight column when viewed form the axis perpendicular to the helical axis. During the sample preparation, significant recoil of the helical structure occurs due to polymer shrinkage which makes the helices prominent in the SEM images. Pang and co-worker report a vertical shrinkage of ~70% at the regions where normal spirals were observed.[21] The recoil characteristics of the helices during polymer shrinkage can be utilized to achieve helices with a much shorter pitch to bring the IR range helical samples to the visible or UV range.

4 Applications

The holographically formed helical structure in H-PDLC has diffractive properties depending on the arrangement of the helical posts and special reflective properties which discriminates circularly polarized light. Both these optical properties can be electrically controlled. This type of film with switchable reflective and diffractive properties has many applications in displays, spectroscopy, lasers, and communication as optical components in the form of polarizers, filters, and anti-reflection coatings.

Outside of optics, the helical structures have a well-controlled porous structure, high surface area to volume ratio, which could be of use as substrates for bio sensors, nano shock absorbers, and for precise nano filtration systems.

5 Conclusion

Thin films with three-dimensional helical microstructures were fabricated in a holographic polymer dispersed liquid crystal. The film has specific reflective and diffractive properties and is a topic worthy for further scientific investigation for new electro-optical devices and applications. The physical dimensions of the helical posts formed by the holographic method are determined by the wavelength, beam configuration, and the exposure parameters. The formation of helical structures with this technique is investigated with scanning electron microscopy and their diffraction pattern and switching properties are also discussed.

Acknowledgments

This work was supported by the National Science Foundation (EEC-0322878), the Dutch foundation for Fundamental Research on Matter (FOM), and Dutch NanoNed program.

References

1 S R Kennedy *et al*, "Fabrication of tetragonal square spiral photonic crystals," *Nano Lett* **2**(1) 59–62 (2002).
2 O Toader and S John, "Proposed square spiral microfabrication architecture for large three-dimensional photonic band gap crystals," *Science* **292**(5519), 1133–1135 (2001).
3 N Tamaoki, "Cholesteric liquid crystals for color information technology," *Adv Mater* **13**(15), 1135 (2001).
4 D K Yang *et al*, "Cholesteric reflective display -Drive scheme and contrast," *Appl Phys Lett* **64**(15), 1905–1907 (1994).
5 D J Broer, J Lub, and G N Mol, "Wide-band reflective polarizers from cholesteric polymer networks with a pitch gradient," *Nature* **378**(6556), 467–469 (1995).
6 M M Giraudguille, "Twisted plywood architecture of collagen fibrils in human compact-bone osteons," *Calcified Tissue International* **42**(3), 167–180 (1988).
7 F Livolant, "Ordered phases of DNA invivo and invitro," *Physica A* **176**(1), 117–137 (1991).
8 P J Willcox *et al*, "Evidence of a cholesteric liquid crystalline phase in natural silk spinning processes," *Macromolecules* **29**(15), 5106–5110 (1996).
9 D K Yang *et al*, "Control of reflectivity and bistability in displays using cholesteric liquid-crystals," *J Appl Phys* **76**(2), 1331–1333 (1994).
10 A Sullivan, "A solid-state multi-planar volumetric display," *SID Symposium Digest Tech Papers* **34**, 1531–1533 (2003).
11 M F Moreira *et al*, "Cholesteric liquid-crystal laser as an optic fiber-based temperature sensor," *Appl Phys Lett* **85**(14), 2691–2693 (2004).
12 V I Kopp *et al*, "Low-threshold lasing at the edge of a photonic stop band in cholesteric liquid crystals," *Opt Lett* **23**(21), 1707–1709 (1999).
13 A Hochbaum *et al*, "Cholesteric color filters: Optical characteristics, light recycling, and brightness enhancement," *SID Symposium Digest Tech Papers* **20**, 1063–1065 (1999).
14 J Schmidtke *et al*, "Laser emission in a dye doped cholesteric polymer network," *Adv Mater* **14**(10), 746 (2002).
15 A L Elias *et al*, "Template induced chiral ordering in nematic liquid crystalline materials: A deuterium nuclear magnetic resonance study," *J Appl Phys* **99**(11) (2006).

16 K Robbie *et al*, "Ultrahigh vacuum glancing angle deposition system for thin films with controlled three-dimensional nanoscale structure," *Review of Scientific Instruments* **75**(4), 1089–1097 (2004).
17 S Maruo, O Nakamura, and S Kawata, "Three-dimensional microfabrication with two-photon-absorbed photopolymerization," *Opt Lett* **22**(2), 132–134 (1997).
18 K K Seet *et al*, "Three-dimensional horizontal circular spiral photonic crystals with stop gaps below 1 μm," *Appl Phys Lett* **88**(22), 3 (2006).
19 K K Seet *et al*, "Three-dimensional circular spiral photonic crystal structures recorded by femtosecond pulses," *J Non-Crystalline Solids* **352**(23–25), 2390–2394 (2006).
20 K K Seet *et al*, "Three-dimensional spiral-architecture photonic crystals obtained by direct laser writing," *Adv Mater* **17**(5), 541 (2005).
21 Y K Pang *et al*, "Chiral microstructures (spirals) fabrication by holographic lithography," *Optics Express* **13**(19), 7615–7620 (2005).
22 C C Bowley and G P Crawford, "Diffusion kinetics of formation of holographic polymer-dispersed liquid crystal display materials," *Appl Phys Lett* **76**(16), 2235–2237 (2000).
23 R L Sutherland *et al*, "Bragg gratings in an acrylate polymer consisting of periodic polymer-dispersed liquid-crystal planes," *Chem Mater* **5**(10), 1533–1538 (1993).
24 G P Wang *et al*, "Holography for one-step fabrication of three-dimensional metallodielectric photonic crystals with a single continuous wavelength laser beam," *J Modern Opt* **50**(14), 2155–2161 (2003).
25 Y Yang, S H Zhang, and G P Wang, "Fabrication of two-dimensional metallodielectric quasicrystals by single-beam holography," *Appl Phys Lett* **88**(25), 3 (2006).
26 K A Amundson, van Blaaderen, and P Wiltzius, "Morphology and electro-optic properties of polymer-dispersed liquid-crystal films," *Phys Rev E* **55**(2), 1646–1654 (1997).

Suraj P. Gorkhali received his Sc.M. in 2006 and is expecting to receive his Ph.D. degree in electro-optical engineering in May 2007 from Brown University. He will join FLEXcon, Inc., as Innovations Scientist after completing his studies. His research interests include polarization and amplitude holography, flexible and conformable displays, liquid crystals, and polymers.

Gregory P. Crawford is currently a Professor of Engineering and Physics at Brown University, as well as the Dean of Engineering. His basic research interests include liquid crystals, polymers, and their application in display technology, telecommunications, and medical-device technology. He has over 200 research publications, review articles, and book chapters, and he holds 14 U.S. patents.

Maryna Yemtsova is a Ph.D. student in physics at Radboud University Nijmegen, The Netherlands. She received has M.S. degree in physics from Saint-Petersburg State University, Russia. Her main interest is in electrically and magnetically switchable photonic crystals for linear and nonlinear optics.

Theo Rasing is Professor of physics at Radboud University, Nijmegen, and Director of the Nijmegen Center of Advanced Spectroscopy. His research interests include molecular materials, ultra-fast dynamics of magnetic nanoctructures, and laser manipulation of matter. He has published more than 200 papers.